Robust computation of pulse pressure variations

Soltesz, Kristian

Published in:
Biomedical Signal Processing and Control

DOI:
10.1016/j.bspc.2017.07.021

2018

Document Version:
Peer reviewed version (aka post-print)

Robust computation of pulse pressure variations

Kristian Soltesz[a]

[a]Lund University, Dept. Automatic Control
P.O. Box 118, SE-220 00 Lund, Sweden
E-mail: kristian@control.lth.se

Abstract

Evidence of arterial pulse pressure variations caused by cardio-pulmonary interactions, and their connection to volume status via the Frank-Starling relationship, are well documented in the literature. Computation of pulse pressure variations from arterial pressure measurements is complicated by the fact that systolic and diastolic peaks are not evenly spaced in time. A robust, structurally uncomplicated, and computationally cheap algorithm, specifically addressing this fact, is presented. The algorithm is based on the Lomb-Scargle spectral density estimator, and ordinary least squares fitting. It is introduced using illustrative examples, and successfully demonstrated on a challenging porcine data set.

Keywords— pulse pressure variation, arterial blood pressure, nonuniform sampling, frequency estimation

Highlights

- A method for robust, fast computation of arterial pulse pressure variations, is presented.
- The method is based on the Lomb-Scargle periodogram and least squares regression.
- The algorithm is particularly suitable for closed-loop control, and other time-critical applications.
- A porcine dataset with sudden hemodynamic changes is used to demonstrate feasibility.

1 Introduction

1.1 Cardio-pulmonary variations

One of the earliest descriptions of cardio-pulmonary interaction dates back to 1854, and is due to W. Greisinger. His discovery lay the foundation for A. Kussmaul's 1873 description of the pulsus paradox in his paper *Über schwielge Madiastino-pericarditis und den Paradoxen Puls*[1] [1].

Cardio-pulmonary interactions are a consequence of changes in intrathoracic pressure over the respiratory cycle. The schematic illustration of Figure 1, together with elementary physics, is sufficient to explain these interactions.

A decrease[2] in intrathoracic pressure (during spontaneous inspiration, or the expiratory phase of positive pressure ventilation), results in increased venous return. This is particularly true for the right heart, which receives systemic venous return. The returned blood originates from outside the thorax, and the flow is consequently aided by the decreased intrathoracic pressure. Since the lungs reside within the thorax, the pulmonary venous return, to the left heart, is not affected by

[1]English translation: Concerning calous mediastinopericarditis and the paradoxical pulse.

[2]The use of 'decrease' and 'increase', is with respect to other phases of the respiratory cycle. I.e., we are only considering variations induced by respiration.

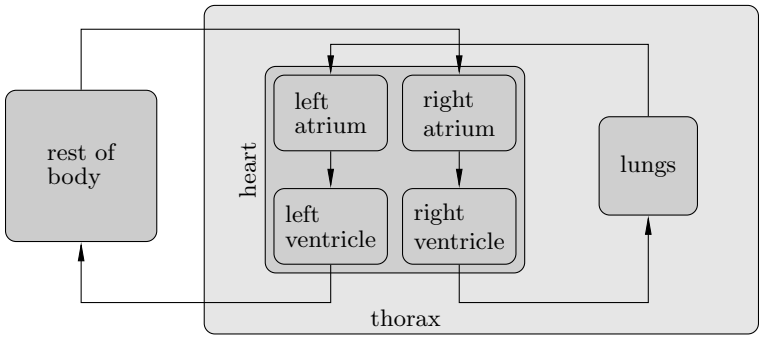

Figure 1: Schematic drawing of the heart and lungs enclosed in the thorax, which can be viewed as a pressure chamber, with pressure variations over the respiratory cycle. The right heart receives systemic venous return from outside the thorax, and ejects the returned blood into the pulmonary circulatory system, residing inside the thorax. The left heart receives pulmonary venous return, from inside the thorax, and ejects the returned blood into the systemic circulatory system, outside the thorax.

this pressure gradient. However, the increased systemic venous return associated with decreased intrathoracic pressure, results in increased pulmonary blood flow, and consequently an increased filling (preload) of the left ventricle. The decreased intrathoracic pressure, increases the load on the left heart, as it is ejecting blood out of the thorax via the aorta. As long as the left heart can cope with this relative increase in afterload, there is an increase in left ventricular stroke volume.

To conclude, the intrathoracic pressure variation over the respiratory cycle results in a left ventricular stroke volume variation, via the cardio-pulmonary interactions described above. While present to some extent during spontaneous breathing, the variation increases notably in patients under positive pressure ventilation. A comprehensive summary of the subject is provided in [2].

The left ventricular stroke volume (SV) is related to arterial pulse pressure (PP), being the difference between systolic and diastolic pressure, through Laplace law. While SV and PP cannot be assumed to be linearly proportional [3], they exhibit a strong correlation. Consequently, stroke volume variations (ΔSV) cause pulse pressure variations (ΔPP[3]) over the respiratory cycle [4]. This is of clinical interest, as measurement of pulse pressure variations, invasively by arterial catetherization, or noninvasively by pulse plethysmograph (PPG) [5], is less complicated than that of stroke volume.

1.2 Pulse pressure variations and hydration status

Evidence linking cardio-pulmonary variations to hydration status was first presented in 1983 [6]. Since then, numerous reports have contributed to strengthen this evidence. It has also been shown that cardio-pulmonary variations constitute a better predictor of hydration status than static parameters, such as central venous pressure. See [7] for a comprehensive review.

The link between cardio-pulmonary variations and hydration status can be explained using the Frank-Starling relationship, conceptually illustrated in Figure 2, and originally due to D. Maestrini (1886–1975), rather than O. Frank and E. Starling, after whom it is named. The curve relates end-diastolic volume to stroke volume of the left heart. As described above, end-diastolic volume varies with intrathoracic pressure over the respiratory cycle, illustrated by vertical grey line pairs. As seen in Figure 2, the magnitude of the corresponding ΔSV is larger at the steep section of the curve, than at the plateau.

Due to the relation between venous return and end-diastolic pressure, the latter is increased if a blood volume expansion is performed through intravenous fluid administration. I.e., volume expansion corresponds to moving to the right in Figure 2, resulting in smaller ΔSV.

One of the main objectives of intravenous fluid management, in intensive care and a majority of surgeries, is to maximize cardiac output (CO) [2], defined as the product of left ventricular stroke

[3]Sometimes PPV is used to denote pulse pressure variations. However, we prefer ΔPP, as PPV can be confused with positive pressure ventilation.

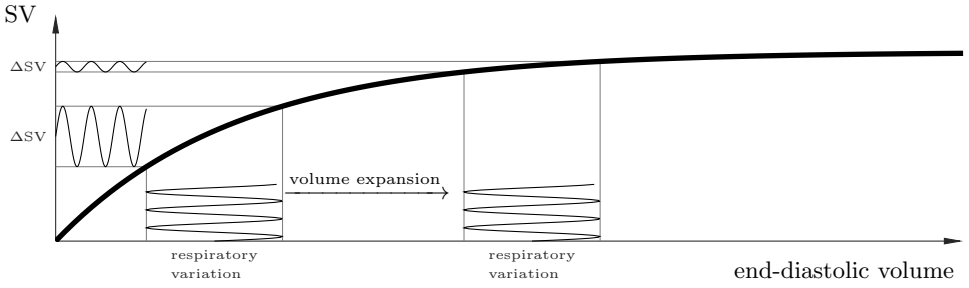

Figure 2: Conceptual illustration of the Frank-Starling relationship between left end-diastolic volume and stroke volume. Volume expansion shifts the interval, across which intrathoracic pressure varies over each respiratory cycle, to the right, thereby decreasing ΔSV and consequently ΔPP.

volume and heart rate. Consequently, it is motivated to perform volume expansion until the plateau of the Frank-Starling curve of Figure 2 is reached. Once the plateau is reached, further volume expansion only marginally increases stroke volume, and consequently cardiac output. Relatedly, further volume expansion may lead to hyperhydration, with adverse effects, including increased mortality in some patient groups, as described in e.g., [8]. Exploiting the previously mentioned correlation between ΔSV and ΔPP, the rationale is therefore to perform volume expansion, as long as it results in decreased ΔPP.

1.3 Pulse pressure variation algorithms

There exist several commercial monitors, which compute cardio-pulmonary variation indices, such as ΔPP, with the intention to guide clinicians in the titration of intravenous fluids. Most of these monitors, including the PiCCO (Pulsion Medical Systems, Feldkirchen, Germany) and FlowTrac (Edwards Life Science, Irvine, CA), utilize propriety algorithm. As pointed out in [7], the availability of open algorithms is essential for the research community. This is particularly true for research on closed-loop controlled fluid management systems [9, 10], where dynamics of the monitor influence the closed-loop system; its performance, robustness, and ultimately even its stability.

While there exist a multitude of algorithms for estimation of respiratory rate from PPG in spontaneously breathing individuals [11], there exist few published algorithms for the computation of pulmonary variation indices in mechanically ventilated patients. A notable exception is the algorithm published in [12], and implemented in the Philips Intelivue MP70 (Philips Medical System, Suresnes, France). That algorithm relies on peak detection, with subsequent estimation of enveloping functions. Unlike the algorithm to be proposed herein, it relies on uniform resampling of data, does not impose structure (e.g., sinusoidal) on the envelopes, and does not define pulse pressure between beats.

1.4 Robust computation of pulse pressure variations

A simple algorithm for fast online computation of arterial pulse pressure variations (ΔPP) will be introduced, demonstrated, and discussed. The algorithm has few parameters, which all have intuitive interpretations, enabling the recommendation of sound default values. It is robust to outliers, and provides a measure of its output confidence. Minimal example implementations in the Matlab programming language can be downloaded from [13].

Demonstration of the algorithm is performed using porcine arterial pressure data, sampled at 100 Hz by catetherization of the ascending aorta. The data was acquired as part of a closed-loop hemodynamic stabilization project. Experimental conditions and compliance with ethical standards were reported in [14]. Details concerning study ethics are additionally found at the end of this paper, under "Compliance with ethical standards". Cardiovascular similarities between human physiology and porcine models [15], support the thesis that successful demonstration of the proposed algorithm in a porcine model indicates applicability to human arterial pressure data.

2 Algorithm

This section presents a robust, simple, and computationally cheap algorithm for computation of ΔPP (%), defined through:

$$\Delta\mathrm{PP} = 100 \cdot \frac{\mathrm{PP}_{\max} - \mathrm{PP}_{\min}}{\mathrm{PP}_{\mathrm{mean}}}, \tag{1}$$

where the max, min, and mean of the pulse pressure signal, PP, are taken over a historic window, with a duration T, exceeding the respiratory period.

Computation of ΔPP is complicated by the fact that PP is traditionally defined as the difference between consecutive systolic and diastolic arterial pressure peaks. Hence, it is only defined at discrete instances, coinciding with heart beats, and consequently not periodically spaced. To circumvent this problem, a continuous time signal $\hat{y}_s(t)$ is fitted to the systolic and diastolic peak signals $y_s(t_s)$, and $y_d(t_d)$, respectively. The algorithm treats $y_s(t_s)$ and $y_d(t_d)$ similarly, and only $y_s(t_s)$ will be considered in the presentation, except when otherwise motivated.

If the patient is under mechanic ventilation, the historic window duration, T, could be chosen as one respiratory period, if known. Otherwise T needs to be chosen sufficiently large to be able to resolve ΔPP, and sufficiently short to render significant hemodynamic changes (blood pressure or heart rate) within the time window improbable. We will utilize a default $T = 10$ s in all examples, and subsequently update T, based on obtained estimates of the respiratory period, as explained later. An alternative, not explored herein, would be the use of a forgetting factor, putting larger emphasis on recent measurements.

A first step toward obtaining $\hat{y}_s$ is to perform peak detection on the continuous arterial pressure signal $y(t)$, to obtain y_s, defined at time instances t_s. Finding $y_s(t_s)$ is readily achievable through prominence-based peak detection, where a reasonable choice of peak prominence is given by $\alpha(\max y(t) - \min y(t))$, evaluated over the considered time window. The parameter α should be chosen sufficiently large not to discard actual systolic peaks, while small enough not to capture local minima. The most prominent local minima are typically the dicrotic waves (visible in Figure 3a), following closure of the aortic valve, occurring approximately at mean arterial pressure [16]. The clinically widespread rule of thumb, that the mean arterial pressure equals diastolic pressure plus one third of the pulse pressure (PP/3), motivates our choice of $\alpha = 1/3$ (used throughout all examples), which eliminates detection of the diacrotic waves by an ample margin.

With $y_s(t_s)$ at hand, $y_d(t_d)$ can be readily obtained, by finding the minima of y between the time instances of t_s.

The role of $\hat{y}_s(t)$ and $\hat{y}_d(t)$ is similar to that of the enveloping functions in [12]. However, rather than simply enveloping the arterial blood pressure signal, we observe that both systolic and diastolic variations follow sinusoidal patterns, as shown in Figure 3. Enforcing this structurally in $\hat{y}_s(t)$ enables a parametric description $\hat{y}_s(t;\theta_s)$, with θ_s being the parameter vector, and the formulation of a parameter fit error, $J_s(\theta_s) = J_s(|\hat{y}_s(t_s;\theta_s) - y_s(t_s)|)$. This has two principal benefits. Firstly, it provides a continuous signal $\hat{y}_s(t)$, which can serve to represent $y_s(t_s)$ at all times within the window. Secondly, $J_s(\theta_s)$ serves as a measure of reliability for the estimate $\hat{\theta}_s$ of θ_s.

Prior to fitting a sinusoid to $y_s(t_s)$, any affine trend $k_s t + m_s$ is removed (with k_s and m_s saved for later use) by ordinary least squares regression, as shown in Figure 3a. Detrending is employed to make the algorithm robust to arterial pressure trends within the considered window T, and we denote the detrended signals with a superscript 0, e.g., $y_s^0(t_s)$.

Fitting of a sinusoid $\hat{y}_s^0(t) = a_s \sin(\omega_r t + \varphi_s)$ to $y_s^0(t_s)$, as shown in Figure 3b, is conducted in two steps. First, the respiratory angular frequency, ω_r, is estimated. The use of standard power spectral techniques such as fast Fourier transform (FFT) is limited by $y_s^0(t_s)$ not being uniformly sampled. Even if it were (e.g., as a result of interpolating resampling), the short window length, T, would not provide sufficient frequency resolution within the band of interest.

Both above problems can be resolved by employing the Lomb-Scargle spectral estimator [17]. The underlying method is also known as least-squares spectral analysis (LSSA). It is closely related to the FFT, but has the advantages of not relying on uniformly sampled data, and being able to compute spectral power density (PSD) estimates at isolated frequencies, rather than over frequency intervals. Its PSD estimate, at the angular frequency ω, for a zero-mean signal $x(t)$, e.g., $y_s^0(t_s)$,

indexed by k, is provided by

$$\begin{aligned} P_{LS}(\omega) &= \frac{\left(\sum_k x[k]\cos(\omega t[k]-\tau)\right)^2}{\sum_k \cos^2(\omega t[k]-\tau)} + \frac{\left(\sum_k x[k]\sin(\omega t[k]-\tau)\right)^2}{\sum_k \sin^2(\omega t[k])-\tau}, \\ \tau &= \frac{1}{2\omega}\tan^{-1}\frac{\sum_k \sin(2\omega t[k])}{\sum_k \cos(2\omega t[k])}, \end{aligned} \tag{2}$$

where σ^2 is the variance of x, which we can disregard, as we are only interested in finding $\arg\max_\omega P_{LS}(\omega)$.

The PSD estimate P_{LS} is evaluated over a frequency range $\omega_{\min} \leq \omega \leq \omega_{\max}$. In order to avoid folding effects, we enforce a Nyquist frequency corresponding to half the median heart rate during the considered window, $\omega_{\max} = \pi \cdot \text{median}(1/\Delta t_s)/2$. The minimum considered frequency is chosen, assuming T is at least half of the respiratory period: $\omega_{\min} = \pi/T$.

For our purposes we deem it sufficient to evaluate (2) at $N = 64 = 2^6$ uniformly spaced frequencies between $\omega_{\min}$ and $\omega_{\max}$, limits included. The resulting Lomb-Scargle periodogram thus generated by $y_s^0(t)$ of Figure 3b is show in Figure 3c. It has a clear maximum at $\omega = \omega_s$. Similarly, computation of the Lomb-Scargle periodogram for $y_d(t_d)$ yields an angular frequency ω_d. The mean of these is chosen as estimate of the respiratory angular frequency, $\hat{\omega}_r = (\omega_s + \omega_d)/2$.

If the respiratory period is a priorily known to the algorithm, $\hat{\omega}_r = \omega_r$, the use of the Lomb-Scargle PSD estimator becomes superfluous. On the other hand, if ω_r is not known a priory, the estimate $\hat{\omega}_r$ can be additionally used to update the window duration, T. We have utilized the update $T := 1.5 \cdot 2\pi/\hat{\omega}_r$, where the factor 1.5 is in place to ensure a sufficiently long window for the Lomb-Scargle estimator to robustly determine $\hat{\omega}_r$ in the next iteration.

With $\hat{\omega}_r$ at hand, it is straightforward to fit the amplitude, a_s and phase φ_s of the systolic variation $\hat{y}_s^0(t) = a_s \sin(\hat{\omega}_r t + \varphi_s)$, by solving

$$\min_{a_s,\varphi_s} \|y_s^0 - \hat{y}_s^0\|_2^2 = \sum_k \left| y_s^0(t_s[k]) - a_s \sin(\hat{\omega}_r t_s[k] + \varphi_s) \right|^2. \tag{3}$$

The problem (3) can be reformulated as

$$\min_{x_1,x_2} \|x_1 \cos(\hat{\omega}_r t_s) + x_2 \sin(\hat{\omega}_r t_s) - y_s^0(t_s)\|_2^2, \tag{4}$$

which is an ordinary least squares problem in $x = \begin{bmatrix} x_1 & x_2 \end{bmatrix}^T$, relating to (3) through

$$\begin{aligned} a_s &= \|x\|_2, \\ \varphi_s &= \text{atan2}(x_1, x_2). \end{aligned} \tag{5}$$

The estimated pulse pressure signal, $\hat{y}_{\text{PP}}(t)$, defined over the window $0 \leq t \leq T$, is the difference between the fitted signals,

$$\hat{y}(t) = \hat{y}_s(t) - \hat{y}_d(t). \tag{6}$$

It can be expressed as the sum of a sinusoid and an affine function

$$\hat{y}(t) = a \sin(\hat{\omega}_r t + \varphi) + kt + m, \tag{7}$$

where

$$\begin{aligned} a &= \sqrt{(a_s \cos\varphi_s - a_d \cos\varphi_d)^2 + (a_s \sin\varphi_s - a_d \sin\varphi_d)^2}, \\ \varphi &= \tan^{-1}\left(\frac{a_s \sin(\varphi_s) - a_d \sin(\varphi_d)}{a_s \cos(\varphi_s) - a_d \cos(\varphi_d)}\right), \\ k &= k_s - k_d, \\ m &= m_s - m_d. \end{aligned} \tag{8}$$

Note that the algorithm allows for $\varphi_s - \varphi_d \neq 0$, to cater for the possibility that the phase of the cardio-pulmonary interaction signals is not identical in systole (y_s^0) and diastole (y_d^0). The mean pulse pressure can now be computed as

$$\text{PP}_{\text{mean}} = \frac{1}{T}\int_0^T \hat{y}(t)dt = \frac{a}{T\hat{\omega}_r}(\cos(\varphi) - \cos(\varphi + T\hat{\omega}_r)) + \frac{kT}{2} + m. \tag{9}$$

The extrema of the pulse pressure variation signal fulfill

$$\begin{aligned} \frac{d}{dt}\hat{y}(t) = 0 \Leftrightarrow t = t_0 + \frac{2\pi m}{\hat{\omega}_r}, \\ t_0 = \frac{\pm\cos^{-1}\left(-\frac{k}{a\hat{\omega}_r}\right) - \varphi}{\hat{\omega}_r}, \ : m \in \mathbb{Z}. \end{aligned} \tag{10}$$

Consequently, $\mathrm{PP}_{\min}$ and $\mathrm{PP}_{\max}$ are found at either of the two smallest or largest t solving (10) withing the considered window $0 \leq t \leq T$, or at the endpoints $t \in \{0, T\}$. The mentioned solutions are given by any $0 \leq t \leq T$ fulfilling $t = \mod(t_0, 2\pi/\hat{\omega}_r) := t_0$ and $t = t_0 + \lfloor\hat{\omega}_r(T - t_0)/(2\pi)\rfloor 2\pi/\hat{\omega}_r$, respectively. (Here, 'mod' is the real modulo function mapping $\mathbb{R}^2 \to \mathbb{R}$.)

2.1 Quality of fit

We use the relative mean square (RMS) error to quantify fit error:

$$J_s = RMS(\frac{\hat{y}_s - y_s}{a_s}) = \left\| \frac{\hat{y}_s - y_s}{a_s \# y_s} \right\|_2 = \sqrt{\frac{1}{a_s \# y_s}(\hat{y}_s - y_s)^\top(\hat{y}_s - y_s)}, \tag{11}$$

where $\# y_s$ denotes the number of points in y_s, and J_d is defined analogously. The fit error of (11) is proportional to the $\mathcal{L}_2$ error of the ordinary least squares problem used to obtain the fit. Scaling by the fit amplitude and number of data points are in place, in order to enable comparison between fits for data sets of unequal size, and with varying degree of underlying cardio-pulmonary interaction, respectively.

2.2 Computational efficiency

The proposed algorithm is computationally cheap, as it relies solely on evaluation of trigonometric functions, and the numeric linear algebra necessary to perform ordinary least squares regression. A non-optimized Matlab implementation [13] computes ΔPP within 0.01 s[4]. Due to its short execution time, the algorithm is suitable for real-time implementation in a desktop computer, and in most modern embedded platforms. Furthermore, the algorithm exhibits moderate dimensional complexity. Peak detection, periodogram computation and maxima location are all $\mathcal{O}(n^2)$, n being the input data dimension. Least squares regression is also $\mathcal{O}(n^2)$, making the entire algorithm $\mathcal{O}(n^2)$.

3 Evaluation

To investigate feasibility of the proposed algorithm, it was evaluated on data collected during the first of two experiments, reported in [14]. Diastolic, y_d, and systolic, y_s, values of a one hour section of arterial blood pressure data, sampled at 100 Hz, is shown in Figure 4a. The particular data segment was chosen, due to the presence of several rapid arterial pressure changes, which potentially pose a challenge for the proposed algorithm. The pulse pressure variation signal, ΔPP, is shown in Figure 4b (grey). Clearly, high frequency components of the signal– corresponding to time constants in the minute or sub-minute range – do not reflect changes in volume statue. This motivates low-pass filtering, prior to using the signal for volume assessment purposes. For demonstration purposes, a filtered version of the raw ΔPP signal, utilizing the zero-order-hold sampled equivalent of the continuous time low-pass filter low-pass filter $1/(sT+1)^2$ with $T = 5$ min time constant, has been added to Figure 4b (black).

Figure 4c shows the relative angular frequency estimation error, $(\hat{\omega}_r - \omega_r)/\omega_r$, with mean and standard deviation of 0.06 and 2.5 %, respectively.

The dataset of Figure 4 was obtained from a ventilator dependent pig under positive pressure mechanical ventilation (Servo Ventilator 300; Siemens AB, Solna Sweden). The ventilator was operated in volume-controlled pressure regulated mode, with a minute volume of 100-150 ml/(kg

[4]Matlab R2016b (9.0.0.341369) on 1.2 GHz Intel core m5 wit 8 Gb RAM.

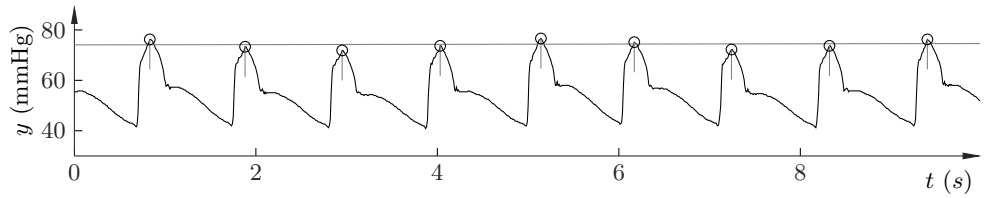

(a) Arterial pressure signal, $y(t)$, detected systolic peaks, $y_s(t_s)$, and affine trend $k_s t + m_s$. Vertical lines indicate by how much the prominence threshold $\alpha(\max(y) - \min(y))$ was exceeded.

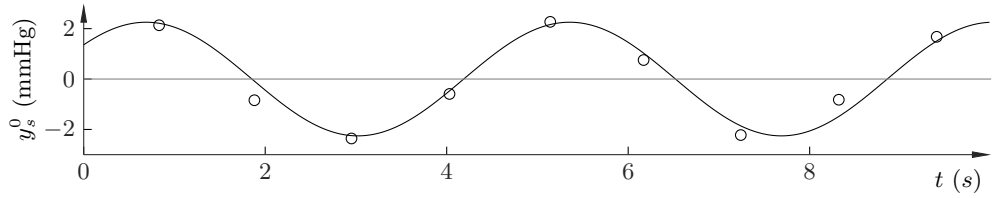

(b) Detrended systolic peak signal $y_s^0(t_s)$, and least equares fit $\hat{y}_s^0(t) = a_s \sin(\hat{\omega}_r t + \varphi_s)$.

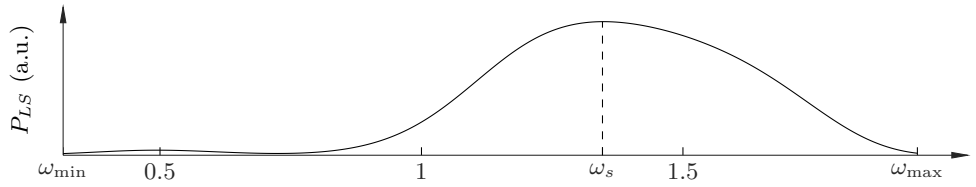

(c) Lomb-Scargle periodogram for $y_s^0(t_s)$, with maximum at ω_s.

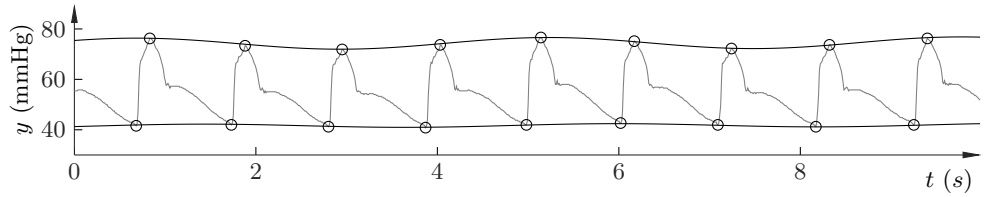

(d) Fitted systolic and diastolic signals $\hat{y}_s(t)$ and $\hat{y}_d(t)$.

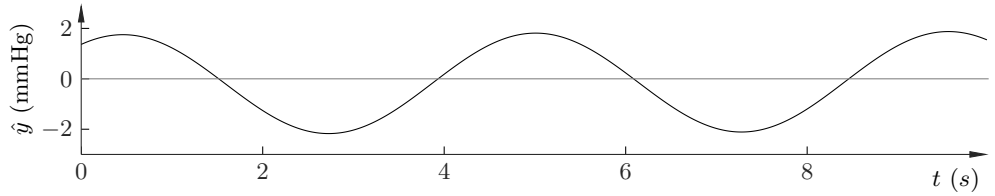

(e) Resulting pulse pressure variation signal $\hat{y}(t) = \hat{y}_s(t) - \hat{y}_d(t)$.

Figure 3: Graphical illustration of the proposed algorithm, using a representative arterial pressure signal $y(t)$, and the proposed window length of $T = 10$ s. Upon detection of systolic peaks (marked with circles), and linear detrending, an estimate of the respiratory angular frequency $\hat{\omega}_r$ is obtained using the Lomb-Scargle spectral estimator. The corresponding amplitude and phase of the systolic pressure variations due to respiration, are determined using ordinary least squares. The same procedure is undertaken for diastolic peaks to arrive at the pulse pressure variation signal.

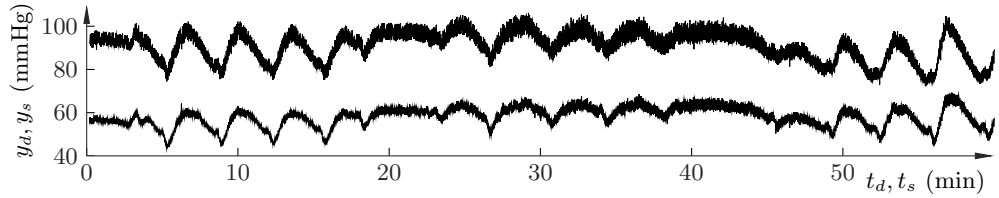

(a) Diastolic, $y_d(t_d)$ (lower), and systolic, $y_s(t_s)$ (upper), arterial blood pressure signals.

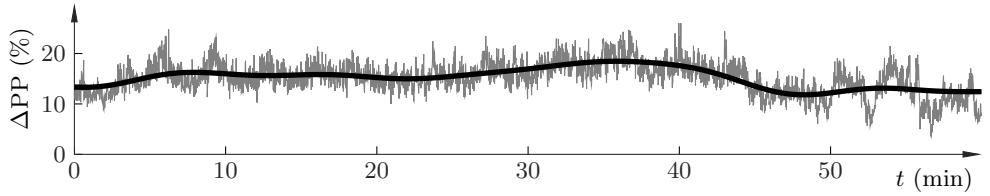

(b) Pulse pressure variation signal, ΔPP (grey), and low-pass filtered version (black).

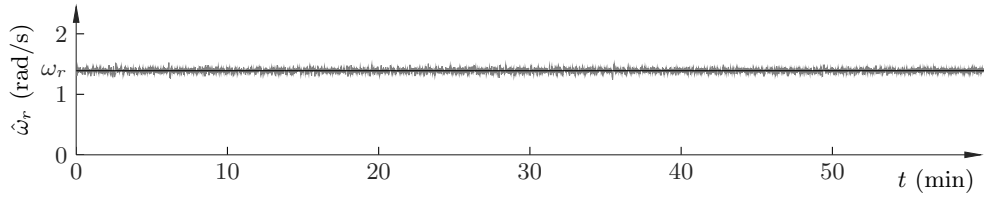

(c) Positive pressure ventilation angular angular frequency, ω_r (black), and estimate, $\hat{\omega}_r$ (grey).

Figure 4: Evaluation of the proposed algorithm on 1 h of arterial pressure data (a), sampled at 100 Hz, and containing several rapid pressure changes. The respiratory frequency is correctly estimated throughout the experiment, as indicated in (c).

body mass) and a positive end-expiratory pressure (PEEP) of 5 cmH_2O. The respiratory cycle was set to 4.5 s, corresponding to the thus known respiratory angular frequency, ω_r. Arterial pressure was measured invasively (DTXPlus; Argon Medical, Plano, TX), and sampled at 100 Hz.

The particular 10 s sequence of Figure 3 was chosen for plotting, based on the fact that the corresponding fit error, J_s, was the one lying closest to the mean of the entire 1 h data set of Figure 4, making it representative of the data set. The worst case J_s was attained for the sequence shown in Figure 5b, resulting in the systolic fit of Figure 5a. The relatively poor fit in this case is caused by the outlier marked '$\times$'. Figure 5 additionally serves to illustrate robustness of the proposed algorithm, which produces a sound fit for all data points except the single outlier. Focusing on J_s, rather than J_d, in this context, is explained by larger respiratory variations in y_s than in y_d, as seen in for example Figure 3 and Figure 5. This renders ΔPP more sensitive to systolic fit errors.

Histograms of the normalized systolic (J_s) and diastolic (J_d) fit errors are shown in Figure 6a, and Figure 6b, respectively. The fits corresponding to the representative sub-sequence shown in Figure 3 are marked with solid vertical line, while the worst-case of Figure 5 is marked with dashed vertical lines.

4 Discussion

The dataset of Figure 4a, used to evaluate the algorithm, was chosen due to its several fast and large arterial pressure changes[5], which pose a challenge to obtainment of the pulse pressure variation signal ΔPP. The good worst-case fit of Figure 5 shows that the algorithm indeed succeeds in robustly and correctly determining ΔPP throughout the dataset of Figure 4a. A secondary indicator of this, confirming the robust performance of the algorithm, is the small (0.06 ± 2.5 %) relative respiratory frequency estimation error.

The interpolative nature of the algorithm can be used to compute both systolic (diastolic)

[5]The changes were drug induced, as explained in [14].

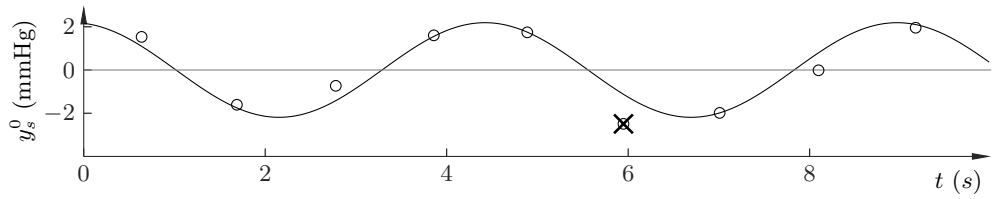

(a) Detrended systolic peak signal $y_s^0(t_s)$, and least squares fit $\hat{y}_s^0(t) = a_s \sin(\hat{\omega}_r t + \varphi_s)$, with outlier marked '×'.

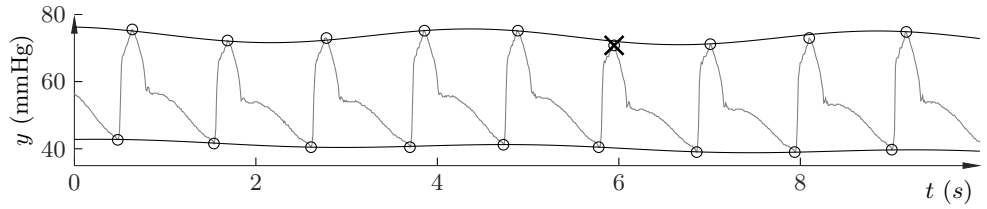

(b) Fitted systolic and diastolic signals $\hat{y}_s(t)$ and $\hat{y}_d(t)$.

Figure 5: The 10 s window producing the worst systolic variation fit within the 1 h data set of Figure 4. The relatively poor fit is due to the outlier marked '×'. (The corresponding diastolic fit lacks such outlier.)

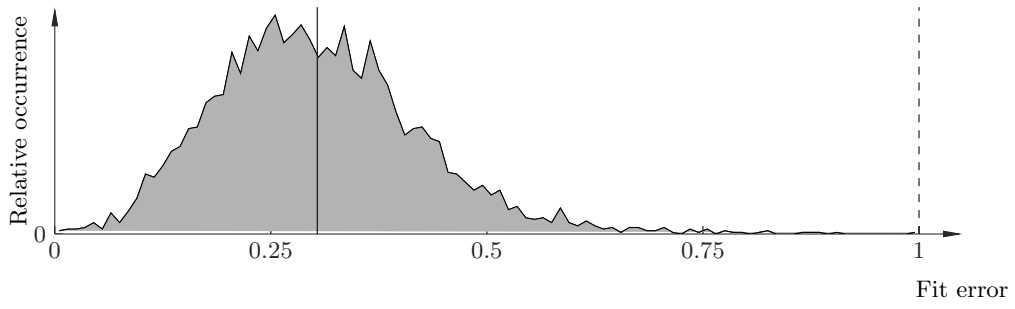

(a) Normalized fit error $(J_s - \min J_s)/(\max J_s)$.

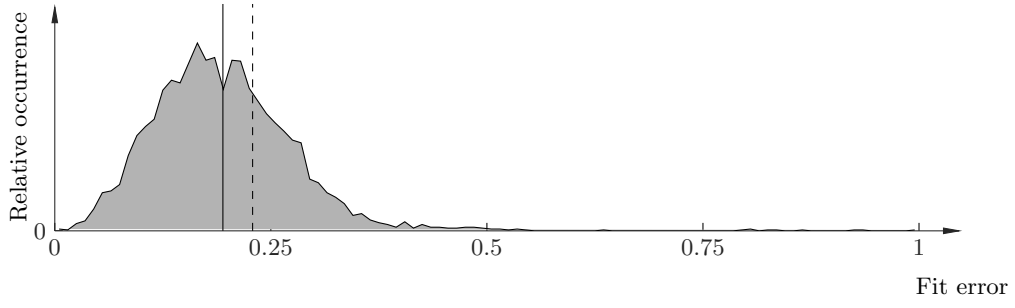

(b) Normalized fit error $(J_d - \min J_d)/(\max J_d)$.

Figure 6: Histograms of the fit errors, as defined by (11). Solid lines correspond to Figure 3 (representative), dashed lines to Figure 5 (worst in data set).

pressure at any time instance t, by evaluating $\hat{y}_s(t)$ ($\hat{y}_d(t)$). Without this feature, the computed ΔPP would depend on the phase between the heart rate and cardiopulmonary interaction signal components, which is obviously undesirable. Relatedly, the interpolation enables displaying or recording the systolic (diastolic) pressure at a uniform sampling rate, rather than at time instances corresponding to the non-uniformly spaced systolic (diastolic) peaks. Furthermore, the algorithm provides the possibility to compensate for the cardiopulmonary interaction when displaying or recording the systolic (diastolic) pressure signals – by subtracting the estimated sinusoid. This feature can easily be implemented also for the mean arterial pressure (MAP).

Alternatively to using $\hat{\omega}_r = (\omega_s + \omega_d)/2$, it would be possible to fit the amplitude and phase using ω_s for the systolic data in (4)–(5) and ω_d for the diastolic. While this could serve to slightly decrease the fit errors J_s and J_d, defined through (11), it would make less physiological sense, as there is *de facto* one true respiratory angular frequency ω_r. It might, however, be that the mean is not the best convex combination of ω_s and ω_d to represent ω_r, depending on what cost $J(J_s, J_d)$ one wishes to minimize. The typically accurate estimation of the respiratory frequency using the mean (see Figure 4c) does, however, not motivate the additional computational cost of finding a $\theta \in [0, 1]$ that minimizes the function J over the convex combination $\hat{\omega}_r = \theta\omega_s + (1 - \theta)\omega_d$.

In addition to computing ΔPP, the computed fit errors J_s and J_d could be used to provide a signal quality index (SQI). In a monitoring or closed-loop control scenario, the ΔPP signal could for instance be discarded whenever some function of J_s and J_d (e.g., $\max(J_s, J_d)$) is larger than a certain threshold. Assuming fixed frequency mechanical ventilation, sudden changes in the estimated respiratory angular frequency $\hat{\omega}_r$ could also be used to lower the SQI.

The low computational cost, together with herein suggested default parameter values, enables straightforward real-time implementation of the algorithm in any desktop computer, and in most embedded systems. Its structural simplicity, makes it readily implementable in virtually any programming language. Furthermore, the low phase lag, determined by the window duration, T, makes the algorithm particularly suitable for providing the input to closed-loop controllers.

The visually observable correlation between the arterial pressures in Figure 4a and the computed pulse pressure variations, ΔPP in Figure 4b, suggest that assessment of volume status based on pulse pressure variations is only reliable if the arterial pressure does not change significantly during the observation period. Relatedly, the observable correlation suggests that ΔPP could be adjusted based on the (mean) arterial pressure, to make ΔPP a more reliable predictor of volume status, in the presence of other hemodynamic changes. In this context, it should be clarified that the purpose of this work was to present a robust algorithm for the computation of ΔPP, rather than to investigate the suitability of pulse pressure variations as a volume status predictor. (The latter has been done by others, as explained in Section 1).

5 Conclusions

An algorithm for computation of the pulse pressure variation signal, ΔPP, based on continuous measurement of arterial pressure, has been proposed. Capability of the algorithm to robustly compute ΔPP, as well as good estimate of respiratory frequency, has been demonstrated on a challenging porcine data set. In addition to ΔPP, the algorithm outputs two fit error signals, which could be used as a signal quality index.

The relevance of ΔPP in the determining of patient volume status, combined with few published algorithms for its computation, suggest usefulness within the research community. The simplicity (example code provided at [13]), high execution speed, and low phase lag, make the algorithm particularly suitable for closed-loop controlled volume expansion.

Acknowledgement

Funding: This work was supported by VINNOVA through the Medtech4Health program (project 2016-01909), and by Hans-Gabriel och Alice Trolle-Wachtmesiters Stiftelse för Medicinsk Forskning. Authors affiliated with Lund University Dept. Automatic Control would like to acknowledge the LCCC and ELLIIT research central. Support was solely in the form of financial funding.

The author would like to acknowledge Stig Steen's group at Igelösa Life Science, for generously sharing their medical knowledge, and the dataset on which the proposed method was evaluated.

Compliance with ethical standards

The animals received humane care in compliance with both EU [18] and US [19] guidelines. The experiments were run under ethic approval M174-15, issued by the *Malmö/Lunds regionala djurförsöksetiska nämnd* (REB).

Conflict of interest

No conflict of interest.

References

[1] S. K. Johnson, R. K. Naidu, R. C. Ostopowicz, D. R. Kumar, S. Bjupati, J. J. Mazza, and S. H. Yale, "Adolf Kussmaul: distinguished clinician and medical pioneer," *Clinical Medicine & Research*, vol. 7, no. 3, pp. 107–112, 2009.

[2] E. A. Williams and G. M. Whitney, "Cardiopulmonary interactions," *Southern African Journal of Critical Care*, vol. 22, no. 1, pp. 28–35, 2006.

[3] R. Bighamian and J. O. Hahn, "Relationship between stroke volume and pulse pressure during blood volume perturbation: A mathematical analysis," *Journal of Biomedicine and Biotechnology*, pp. 1–10, 2014, preprint. DOI: 10.1155/2014/459269.

[4] F. Michard, "Changes in arterial pressure during mechanical ventilation," *Anesthesiology*, vol. 103, no. 2, pp. 419–428, 2005.

[5] M. Cannesson, B. Delannoy, A. Morand, P. Rosamel, Y. Attof, O. Bastien, and J. J. Lehot, "Does the pleth variability index indicate the respiratory-induced variation in the plethysmogram and arterial pressure waveforms?" *Anesthesia & Analgesia*, vol. 106, no. 4, pp. 1189–1194, 2008.

[6] J. P. Coyle, R. S. Teplick, M. C. Long, and J. K. Davison, "Respiratory variations in systemic arterial pressure as an indictor of volume status," *Anesthesiology*, vol. 59, p. A53, 1983.

[7] M. Cannesson, M. Aboy, C. K. Hofer, and M. Rehman, "Pulse pressure variations: where are we today?" *Journal of Clinical Monitoring and Computing*, vol. 25, no. 1, pp. 45–56, 2011.

[8] S. Samoni, V. Vigo, L. I. B. Resendiz, G. Villa, D. S, F. Nalesso, F. Ferarri, M. Meola, A. Brendolan, P. Malacarne, F. Forfori, R. Bonato, C. Donadio, and C. Ronco, "Impact of hyperhydration on the mortality risk in critically ill patients admitted in intensive care units," *Critical Care*, vol. 20, no. 95, pp. 1–8, 2016.

[9] J. Rinehart, N. Liu, B. Alexander, and M. Cannesson, "Closed-loop systems in anesthesia: is there a potential for closed-loop fluid management and hemodynamic optimization," *Anesthesia & Analgesia*, vol. 114, no. 1, pp. 130–143, 2012.

[10] J. Rinehart, C. Lee, C. Canales, A. Kong, Z. Kain, and M. Cannesson, "Closed-loop fluid administration compared to anesthesiologist management for hemodynamic optimization and resuscitation during surgery: an in vivo study," *Anesthesia & Analgesia*, vol. 117, no. 5, pp. 1119–1129, 2013.

[11] P. H. Charlton, T. Bonnici, L. Tarassenko, D. A. Clifton, R. Beale, and P. J. Watkinson, "An assessment of algorithms to estimate respiratory rate from the electrocardiogram and photoplethysmogram," *Physiological Measurement*, vol. 37, no. 4, pp. 610–626, 2016.

[12] M. Aboy, J. McNames, T. Thong, C. R. Phillips, M. S. Ellenby, and B. Goldstein, "A novel algorithm to estimate the pulse pressure variation index deltapp," *IEEE Transactions on Biomedical Engineering*, vol. 51, no. 12, pp. 2198–2203, 2004.

[13] K. Soltesz, "Matlab code for robust computation of pulse pressure variations," git@gitlab.control.lth.se:kristian/DeltaPP.git, 2017.

[14] K. Soltesz, C. Sturk, A. Paskevicius, Q. Liao, G. Qin, T. Sjöberg, and S. Steen, "Closed-loop prevention of hypotension in the heartbeating brain-dead porcine model," *Trans Biomed Eng*, 2016, online Preprint, DOI: 10.1109/TBME.2016.2602228.

[15] Y. Suzuki, C. A. Yeung, and F. Ikeno, "The representative porcine model for human cardiovascular disease," *Journal of Biomedicine and Biotechnology*, vol. 2011, 2010.

[16] J.-L. Hebert, Y. ecarpentier, K. Zamani, C. Coirault, G. Daccache, D. Chemla, N. Wuilliez, and L. Larsonneur, "Relation between aortic dicrotic notch pressure and mean aortic pressure in adults," *The American Journal of Cardiology*, vol. 76, no. 4, pp. 301–306, 1995.

[17] N. R. Lomb, "Least-squares frequency analysis of unequally spaced data," *Astrophysics and Space Science*, vol. 39, no. 2, pp. 447–462, 1976.

[18] The European parliament, "On the protection of animals used for scientific purpose," Council of Europe, Tech. Rep., 2010, directive 2010/63/EU.

[19] National research council of the national academies, "Guide for the care and use of laboratory animals," Institute for laboratory animal research, Tech. Rep., 2011, ISBN 978-0-309-15401-7.